Japanese Journal of Applied Physics
Vol. 43, No. 3, 2004, pp. 1168–1171

Modulation-Free Frequency Stabilization of a Grating-External-Cavity Diode Laser by Magnetically Induced sub-Doppler Dichroism in Cesium Vapor Cell

Junmin WANG*, Shubin YAN, Yanhua WANG, Tao LIU and Tiancai ZHANG

State Key Laboratory of Quantum Optics and Quantum Optics Devices, and Institute of Opto-Electronics, Shanxi University, Taiyuan, Shanxi 030006, P.R.China

(Received September 2, 2003; accepted November 20, 2003; published March 10, 2004)

Thanks to the Zeeman effect and the saturation absorption spectroscopic technique, magnetically induced sub-Doppler dichroism has been experimentally demonstrated in a cesium vapor cell. A dispersion-like frequency-discriminating signal is obtained by this sub-Doppler dichroism. The phase-sensitive detection via lock-in is no longer required because there is no frequency dither on the laser. A grating-external-cavity 852 nm diode laser is frequency-stabilized to cesium $6\ ^2S_{1/2}\ F = 4$–$6\ ^2P_{3/2}\ F' = 4, 5$ crossover by this modulation-free locking scheme. Compared with a frequency fluctuation of approximately 12 MHz under free-running conditions, a typical frequency jitter of less than +/− 260 kHz in 50 s was estimated in the preliminary stabilization. This locking scheme is relatively simple, and it can avoid extra noise due to the direct frequency dither on the laser source in the conventional saturation absorption locking technique. [DOI: 10.1143/JJAP.43.1168]

KEYWORDS: sub-Doppler spectroscopy, magnetically induced dichroism, frequency stabilization, modulation free, cesium atom

1. Introduction

Diode lasers with a stable frequency and a relatively narrow linewidth are required in many fields of research and application. The sensitivity of diode lasers to optical feedback results in an effective reduction in linewidth using a diffraction grating-external-cavity configuration.[1] Atomic or molecular transitions provide a quite stable frequency standard. The conventional absolute frequency stabilization method is well known as the high-resolution saturated absorption spectroscopy technique, which is widely used in the areas of laser spectroscopy, atomic physics, and metrology. To generate a dispersion-like frequency-discriminating signal, requires phase-sensitive detection as a lock-in system, which usually utilizes a small frequency dither on the diode laser directly. More or less, the dither will induce additional noises in the laser frequency and intensity, and it is unacceptable in some applications.

An effective and relatively simple locking method without any frequency dither, known as the dichroic atomic vapor laser lock (DAVLL), was developed by Corwin *et al.*[2] based on the Doppler dichroism induced by a magnetic field on a rubidium vapor cell. Because there is no frequency dither on the laser, no additional noise is introduced and the phase-sensitive detection via lock-in is no longer required. Beverini *et al.*[3] applied this Doppler DAVLL technique to cesium vapor cell. Recently, Wasik *et al.*[4] and Petelski *et al.*[5] demonstrated the sub-Doppler dichroism induced by a weak magnetic field by combining the basic principles of DAVLL and the saturated absorption spectroscopy on sodium and rubidium vapor cells.

In this paper, we extend the sub-Doppler dichroism method to cesium vapor cell and provide the preliminary results of frequency stabilization of an 852 nm grating-external-cavity diode laser by this sub-Doppler dichroism technique. A typical frequency jitter of less than +/− 260 kHz in 50 s was estimated in the preliminary stabilization compared with the frequency fluctuation of about 12 MHz under free-running conditions.

*Corresponding author. E-mail address: wwjjmm@sxu.edu.cn

2. Basic Idea of sub-Doppler Dichroism

Assuming a simple two-level atomic system, the hyperfine ground state with angular momentum $J = 0$ and the hyperfine excited state with $J' = 1$ are schematically shown in Fig. 1. There are three Zeeman sublevels designated as $m_{J'} = -1, 0, +1$ in the excited state, while there is only one Zeeman sublevel $m_J = 0$ in the ground state. Let us consider the configuration of the pump and probe beams both with parallel linear polarizations in the saturated absorption spectrometer, as shown in the dashed-line frame in Fig. 3. The probe beam can be considered as the superposition of two components with different circular polarizations (σ^+ and σ^-). The σ^+ component couples the $m_J = 0$ to $m_{J'} = +1$ transition, whereas the σ^- component couples the $m_J = 0$ to

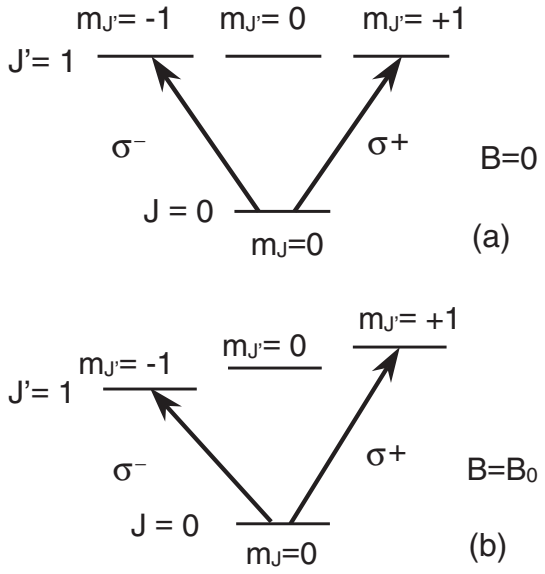

Fig. 1. Two-level atoms model with a hyperfine ground state $J = 0$ and a hyperfine excited state $J' = 1$. In the case of magnetic field $B = 0$, the Zeeman sublevels $m_{J'} = -1, 0, +1$ of $J' = 1$ state are degenerate (a), while a weak uniform magnetic field $B = B_0$ will split the Zeeman sublevels (b). A σ^+ circularly-polarized laser beam will couple $m_J = 0$ to $m_{J'} = +1$ transition, whereas a σ^- circularly-polarized laser beam will couple $m_J = 0$ to $m_{J'} = -1$ transition.

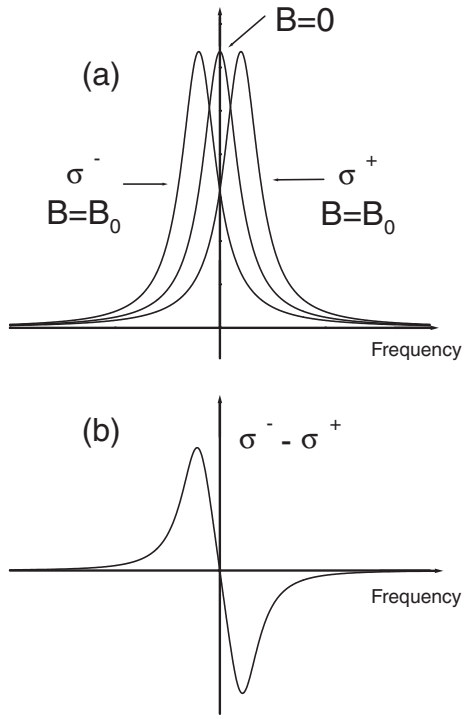

Fig. 2. Saturation absorption spectrum of $J = 0$–$J' = 1$ transition without Doppler background in the cases of magnetic fields $B = 0$ and $B = B_0$ (a). The σ^+ and σ^- components are Zeeman-shifted towards different frequency directions. In other words, the atomic system displays sub-Doppler dichroism. By subtracting the σ^+ and σ^- components, a dispersion-like signal is obtained (b) and it can serve as a frequency-discriminating signal.

$m_{J'} = -1$ transition. In the case of zero magnetic field, all Zeeman sublevels in the excited state are degenerate, as shown in Fig. 1(a). Therefore the σ^+ and σ^- components display their absorption signals at exactly the same frequency locations when the laser scans over the $J = 0$–$J' = 1$ transition. Now we add a uniform weak magnetic field B_0 generated by a solenoid on the atomic vapor cell. The Zeeman effect will break up the degeneration [see Fig. 1(b)]. The corresponding sub-Doppler Lorentz absorption signals of the probe in the case of $B = 0$ and $B = B_0$ are schematically shown in Fig. 2(a), in which the Doppler background is removed. The Zeeman effect results in the splitting of the σ^+ and σ^- components in different frequency locations separated by $\Delta E/h$. ΔE is the splitting between $m_{J'} = +1$ and $m_{J'} = -1$, and is approximately given in the weak field regime as

$$\Delta E = \Delta E(m_{J'} = +1) - \Delta E(m_{J'} = -1) = 2g_{J'} \cdot \mu_B \cdot B_0,$$

where $g_{J'}$ is the Lande factor of the $J' = 1$ hyperfine excited state and μ_B is the Bohr magneton. In other words, the σ^+ and σ^- components of the probe indicate a dichroism under sub-Doppler conditions.

By subtracting the dichroic sub-Doppler Lorentz absorption signals of the σ^+ and σ^- components, the dispersion-like curve can be obtained without any frequency dither on the laser [as shown in Fig. 2(b)]. This dispersion-like curve can serve as the frequency-discriminating signal for the frequency stabilization. To create a proper discriminating signal with a large slope around the zero-crossing point as well as a relatively large frequency capture range which is desired in frequency stabilization, it is reasonable to set the separation of the sub-Doppler Lorentz absorption signals of the σ^+ and σ^- components closer to the linewidth of the saturated absorption line.

In this way, the phase-sensitive detection is no longer required to create the dispersion-like frequency-discriminating signal, so that we are able to stabilize the laser frequency to $J = 0$–$J' = 1$ transition via this sub-Doppler dichroism scheme.

3. Experimental Setup

The schematic diagram of the experimental setup is depicted in Fig. 3. A grating-external-cavity diode laser system operates at the D_2 line of cesium atoms ($6\ ^2S_{1/2}$ F = 4–6 $^2P_{3/2}$) with a typical emission linewidth of approximately about 500 kHz. The laser frequency can be easily controlled either by setting a DC offset voltage on the external-cavity piezoelectric transducer (PZT) between 0 and 100 V or by tuning the injection current. The output beam has been collimated within the laser head, and it passes through a 40-dB optical isolator (OFR IO-HP-850) to avoid optical feedback. Then a tunable beam-splitting unit consisting of a half-wave plate and a polarizing beam-splitting cube (PBS) is used to pick up a small fraction of optical power from the main output beam for the saturated absorption spectrometer.

The pump and probe beams with parallel linear polarizations counter-propagate through a 30-mm-long cesium vapor cell which is placed inside a solenoid driven by a constant current supply. The axis of the solenoid is parallel to the pump and probe beams. Approximately 10 Gauss of magnetic field along the axis of the solenoid is generated by 1 A of current. Two neutral density filters are used to adjust the intensity of the pump and probe beams. In the region of the vapor cell, the pump has a power of approximately 250 μW and a beam size of 2 mm × 3 mm, while the probe has a power of 14 μW and a beam diameter of 1.2 mm. After

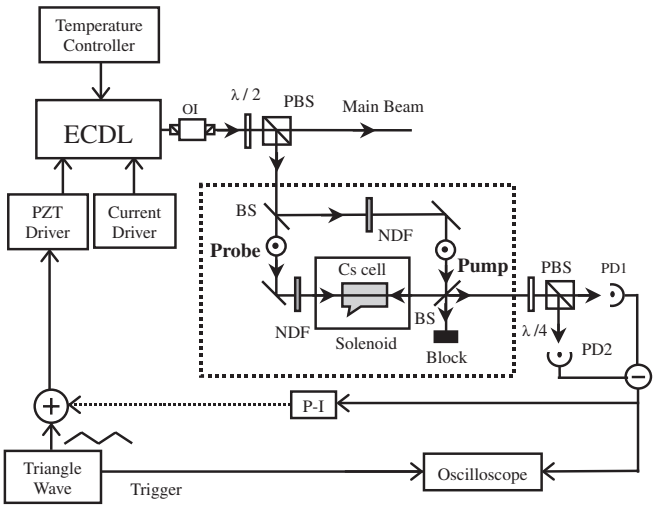

Fig. 3. Schematic diagram of the experimental setup. The dashed-line frame displays the saturation absorption spectrometer. **ECDL**: grating-external-cavity diode laser; **OI**: optical isolator; $\lambda/2$: half-wave plate; $\lambda/4$: quarter-wave plate; **PBS**: polarization beam-splitting cube; **BS**: beam-splitting plate; **NDF**: neutral density filter; **PDs**: photodiodes; **P–I**: proportion and integration amplifier.

the saturation absorption spectrometer, the σ^+ and σ^- components of the probe are separated using a quarter-wave plate and a PBS cube, respectively, then detected by two photodiodes (Hamamatsu S-3399). After subtracting the two signals, a sub-Doppler dispersion-like frequency-discriminating signal will be obtained when the laser scans over the 6 $^2S_{1/2}$ F = 4–6 $^2P_{3/2}$ transition.

Frequency stabilization can be realized by feeding back the error signal with a proper phase to the PZT of the external-cavity diode laser via a proportion and integration (P–I) amplifier. A digital oscilloscope is used to record the dichroic sub-Doppler spectra and to monitor the error signal.

4. Results and Discussion

When the laser scans over 6 $^2S_{1/2}$ F = 4–6 $^2P_{3/2}$ F′ = 3, 4 and 5 transition of the cesium D_2 line, the dichroic sub-Doppler spectra measured by the two photodiodes are shown in Fig. 4. The hyperfine peaks corresponding to the σ^+ and σ^- components of the probe separate according to the prediction of the sample model in §2. The typical linewidth of the hyperfine transitions or the crossovers is approximately 15 MHz, which is somewhat larger than the natural linewidth of 5.3 MHz, and this is mainly due to power broadening. A dispersion-like structure for F = 4–F′ = 5 transition is observed in upper curve (also see the inset).

By subtracting the dichroic sub-Doppler spectra, a frequency-discriminating signal is obtained (Fig. 5). We reasonably choose the crossover F = 4–F′ = 4 and 5 as our reference frequency standard. The slope around the zero-crossing point is estimated by the peak-to-peak frequency span of the dispersion-like structure of the F = 4–F′ = 4 and 5 crossover, which is calibrated by the hyperfine splitting of the 6 $^2P_{3/2}$ state. Thus, the amplitude of the frequency error signals under free-running conditions as well as after locking can be approximately converted into frequency jitters.

To estimate the frequency fluctuation, the laser is tuned to the reference standard, then left free-running. A typical frequency fluctuation is shown in Fig. 6(a). Record time is 50 s, which is limited by the digital oscilloscope used in the experiment. The estimated frequency jitter is approximately 12 MHz. A semiperiodic jitter of approximately 100 Hz may be due to the mechanical noise from the cooling fan inside the laser head and the fluctuation of the 220 V AC power supply.

After closing-loop locking, the frequency fluctuation is clearly suppressed. Within 50 s, a typical frequency fluctua-

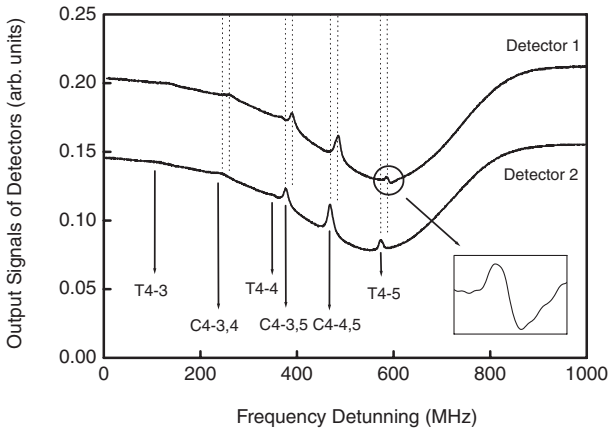

Fig. 4. Saturation absorption spectra of cesium 6 $^2S_{1/2}$ F = 4–6 $^2P_{3/2}$ transition for σ^+ and σ^- components of the probe with a weak magnetic field. All hyperfine transitions and crossovers for σ^+ and σ^- components are Zeeman-shifted.

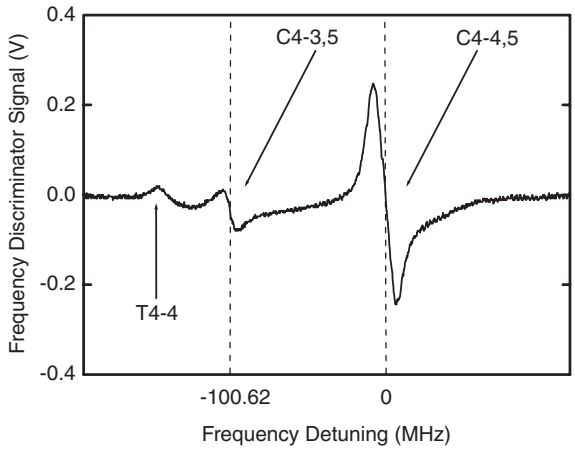

Fig. 5. Dispersion-like frequency-discriminating signal. The F = 4–F′ = 4, 5 crossover is selected reasonably as a reference standard for frequency stabilization. The horizontal axis is calibrated by the hyperfine splitting of the 6 $^2P_{3/2}$ state.

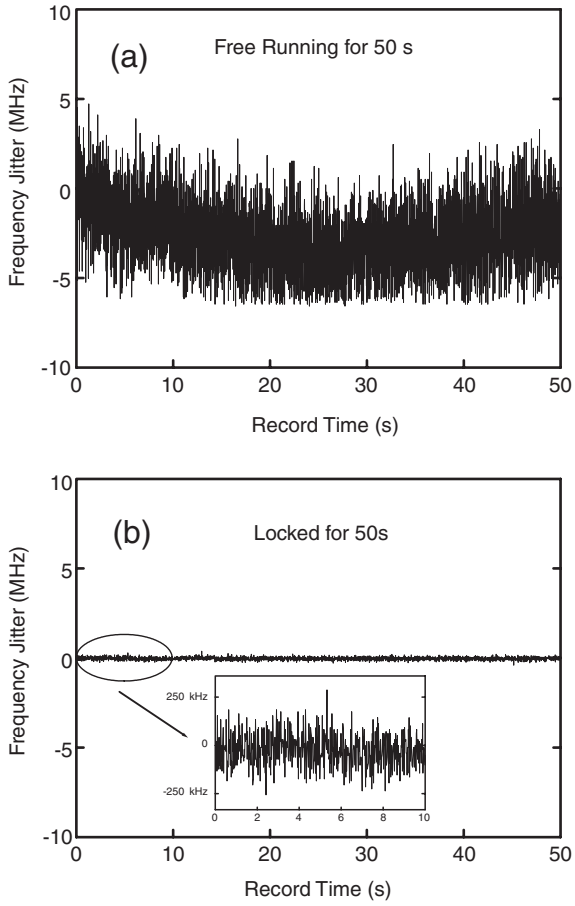

Fig. 6. Typical frequency error signals in the case of free running (a) and locking (b). Within 50 s, the frequency jitter for free running is about 12 MHz. After locking, the residual frequency jitter is estimated to be less than +/− 260 kHz in the preliminary stabilization.

tion is shown in Fig. 6(b) and the estimated frequency jitter is less than +/− 260 kHz in the preliminary stabilization. The inset shows 10 s of record time. Actually, the grating-external-cavity diode laser can be locked over several hours. Accurate evaluation of the frequency stability can be carried out by the beat-note technique. This was not attempted in our experiment. Furthermore, we will improve the frequency stability by means of feeding back the fast components of the error-correcting signal to the current modulation channel of the diode laser. This will enhance the response ability of the stabilization loop because the injection current has a much larger frequency bandwidth (DC ∼400 kHz) than the PZT of the external cavity (DC ∼2 kHz).

In conclusion, the sub-Doppler dichroism induced by a magnetic field has been demonstrated in a cesium vapor cell. Using the simple sub-Doppler dichroism scheme, a grating-external-cavity diode laser system is frequency-stabilized to the cesium D_2 line without any frequency dither on the laser. An estimated frequency jitter of less than +/− 260 kHz is obtained in the preliminary stabilization.

Acknowledgments

The authors are very grateful to Prof. Kunchi PENG and Prof. Changde XIE for stimulating discussions and encouragements. Thanks to other members of the C-QED group for their contributions to this work at different stages. This project is partially supported by the National Natural Science Foundation of China (approval numbers: 60178006 and 10374062), by the Natural Science Foundation of Shanxi Province (approval number 20021030), and by the Research Fund for Returned Scholars Abroad of Shanxi Province.

1) C. E. Wieman and L. Hollberg: Rev. Sci. Instrum. **62** (1991) 1.
2) K. L. Corwin, Z. T. Lu, C. F. Hand, R. J. Epstein and C. E. Wieman: Appl. Opt. **37** (1998) 3295.
3) N. Beverini, E. Maccioni, P. Marsili, A. Ruffini and F. Sorrentino: Appl. Phys. B **73** (2001) 133.
4) G. Wasik, W. Gawlik, J. Zachorowski and W. Zawadzki: Appl. Phys. B **75** (2002) 613.
5) T. Petelski, M. Fattori, G. Lamporesi, J. Stuhler and G. M. Tino: Eur. Phys. J. D **22** (2003) 279.